Journal for Research in Applied Sciences and Biotechnology
www.jrasb.com

ISSN: 2583-4053
Volume-1 Issue-5 || December 2022 || PP. 188-194
https://doi.org/10.55544/jrasb.1.5.20

Effect of Elements (Mo, Zr) on a Copper-Based Alloy to Attenuate X-Rays

Fareed Majeed Mohammed[1], Raed Najeeb Razooqi[2] and Mahmood Abrahim Mahmed[3]
[1]College of Science, Department of Physics, Tikrit University, REPUBLIC OF IRAQ.
[2]College of Engineering, Department of Mechanics, Tikrit University, REPUBLIC OF IRAQ.
[3]College of Science, Department of Physics, Tikrit University, REPUBLIC OF IRAQ.

[1]Corresponding Author: alkese015@gmail.com

www.jrasb.com || Vol. 1 No. 5 (2022): December Issue

Received: 29-11-2022 **Revised:** 20-12-2022 **Accepted:** 29-12-2022

ABSTRACT

Copper-based alloys were prepared by powder metallurgy technique (Cu +5%Al +3%Ti) to measure the attenuation coefficients of X-rays for a range of operating voltages (20,25,30,35) kV with variable thickness (0.2 - 0.6)Cm at constant compressive pressure (600Mpa) according to the order (A1, A2, A3, A4, A5), variable percentages of molybdenum and zirconium (X=1,2,3,4,5) were added separately to the allo (Cu 92-x + 5%Al +3%Ti + Mo x) in the order (B1,B2,B3,B4,B5), and allo (Cu92-x + 5%Al + 3%Ti + Zr x) in the order (C1,C2,C3,C4,C5) with a thickness of (0.6 Cm) and a pressure of (600Mpa), all samples were sintered at a temperature of (900 ^{0}C) for a period of (4 hours).

The results show that at an operating voltage of (20Kv), the linear and mass attenuation coefficients increased by (47%) (61.8%), the Hardness increased by (30%), and the porosity decreased by (13.3%) when comparing the results of Alloys (A1) with (A5). Results The attenuation coefficients increased when adding the molybdenum element by (31.3%) (30%), the Hardness increased by (22.3%), and the porosity decreased by (33.5%) when comparing the results of Alloys (B1) with (B5).

The decrease in the attenuation coefficients when zirconium was added in proportions (28.5%) (25.6%), and the Hardness decreased by (11.4%). The porosity increased by (15%) when comparing the results of Alloys (C1) with (C5). The attenuation coefficient is inversely proportional to the operating voltage. It decreased by (29.4%) when comparing the results of voltages (20Kv) with (35Kv) for alloy (B5) and by (36%) for alloy (C5).

Keywords- smart alloys, linear and mass attenuation coefficient, Hardness, porosity, operating voltage.

I. INTRODUCTION

The scientist (Barclay) is the first to conduct attenuation experiments for X-rays during their passage through absorbent materials such as carbon. He found that the energy of these rays dissipates and weakens, meaning that the electrons of these materials work to disperse part of the energy of the incident beam of radiation, as the photons of the beam suffer multiple collisions during its passage. It suffers from reflection, refraction, and diffraction at different angles. All of these processes weaken the particle intensity with the distance it travels and the atomic number of the materials through which the radiation beam passes. This process is called attenuation [1, 2].

The effectiveness of the material envelopes is calculated by the interactions with the rays falling on them and the absorption process. To improve the shielding effectiveness, alloys and composite materials are resorted to that provide additional advantages in resistance and durability in addition to the ability to attenuate or weaken the radiation carried out by the alloys [3,4].

II. ATTENUATION

When a beam of X-ray photons falls on the surface of a material, each Photon in this beam either interacts with the medium, the surface of the attenuated material, through absorption and scattering interactions,

ISSN: 2583-4053
Volume-1 Issue-5 || December 2022 || PP. 188-194
www.jrasb.com
https://doi.org/10.55544/jrasb.1.5.20

or does not interact at all. There is an attenuation of its energy (Energy attenuation) or an attenuation of its intensity (intensity attenuation), since the energy or intensity decreases along the path that the beam travels through the attenuated medium, as there are three main processes of interaction (X-rays) with the matter, which are the photoelectric phenomenon, Compton scattering, and pair production, As the sum of the operations is called the linear attenuation coefficient (μL) and is given by the following relationship [5].

$$\mu_L = \sigma(\text{photoelectric}) + \sigma(\text{Compton}) + \sigma(\text{pair}) \;.....(1)$$

σ = cross-sectional area of the reaction

The linear attenuation coefficient is measured in units of (Cm-1, mm-1). It depends on the thickness of the material (X (cm, mm)), the energy of the incident photon, and the atomic number (Z) of the material. It is given by the following relationship [6]:

$$\mu_L = \frac{ln\frac{I.}{I}}{X} \;............... (2)$$

The mass attenuation coefficient (μ_m) is measured in units of (cm².gm-1), and is given by the following relationship [6]

$$\mu_m = \frac{ln\frac{I.}{I}}{\rho X} \;.........................(3)$$

Since the discovery of X-rays, researchers have resorted to studying and measuring the attenuation of these rays because of the practical importance of these results in different fields. Some studies come in the attenuation of X-rays as the radiation source in our research. In 2011, the researcher (Farid et al.) presented a study to measure Linear and mass x-ray attenuation coefficients for aluminum-based alloys, as it was found that the relationship is inverse between particle size and attenuation coefficients [7]. In 2012, the researcher (Farid et al.) presented a practical study on the effect of oxidation of aluminum-based alloys on the linear and mass attenuation coefficients for the operating voltage range of (20-35)Kv, as it was found that the relationship is direct between the attenuation coefficients and the oxidation time of the alloys, and is inverse with the voltage Employment [8]. In 2014, the researcher (Farid et al.) conducted a practical study to measure the effect of the thickness of the samples on the attenuation coefficients of X-rays for the elements (Cu, Ti, Zn, Al), as he found that the relationship is direct between the coefficients of attenuation, thickness, and Hardness with the coefficients of attenuation [9]. In 2017 The researcher (Oasarmo, Vishal. V, and others) studied the attenuation coefficients, the half-thickness, and the free path rate of some shape memory alloys for the energy range (122-1330) Kev, as the study showed the dependence of the variation of the values obtained for all parameters on the photon energy [10].In (2018), the researcher Dapke Gopinath (P et al) conducted several studies on the cross-section parameters of the attenuation of some memory alloys for shape in the energy range 356 -1330 (Kev), and it was found that there is a good agreement between the experimental and theoretical values of the mass attenuation coefficient of the memory alloys (SMA), which are (Al Ni), (Fe Ti), (Cu Zn), (Cu Sn), and (Fe Cr Ni MO) in addition to experimentally obtaining some relevant parameters using the values obtained from the attenuation coefficients at the power of Photon (356 - 1330 Kev) [11]. In 2018, the researcher (Farid et al.) presented a study to measure the X-ray attenuation coefficients for (Cu, Zn) and lead alloys of different thicknesses [12]. In 2021, the researcher (Farid et al.) studied the effect of shape memory alloys used as protective shields from radiation effects in terms of attenuation coefficients. The shape memory alloy was prepared using powder metallurgy technology and by increasing the pressure of cold pressing during preparation from (100 - 500) Mpa at a thickness of (0.4Cm) increased Hardness and decreased porosity, in addition to increasing linear and mass attenuation coefficients when exposed to atomic and nuclear radiation [13]. In 2022, the researcher (Farid et al.) studied the X-ray attenuation of the voltage range (20-35) kV for smart alloys based on copper by adding nanoparticles and microparticles of silver, as the shape memory alloy was prepared by powder metallurgy technique and by increasing the pressure of cold pressing during preparation From (200-600)Mpa at a thickness of (0.6 cm), the Hardness increased. The porosity decreased, in addition to increasing the linear and mass attenuation coefficients when exposed to atomic radiation [14].

III. MEMORY ALLOYS FOR SHAPE

Shape memory alloys (SMAs) have wide applications in thermal sensors, protection devices, medical devices, and others due to their unique properties such as Super Elasticity, and the shape memory effect (SMAs), and to improve their properties, limited quantities of some alloying elements are added to them individually or jointly. The basis of the effect is the transformation of the alloys from the martensite phase to another austenite phase when it is heated to high temperatures and returned to its original shape after cooling, [15, 16].

IV. EXPERIMENTAL PART

1- Preparation of samples

The alloys of our current research were prepared using powder metallurgy technology by weighing the components of the alloy according to the volumetric proportions using an electronic balance. The

ISSN: 2583-4053
Volume-1 Issue-5 || December 2022 || PP. 188-194
https://doi.org/10.55544/jrasb.1.5.20

alloys were coded as shown in Table (1), and the components of each sample were ground and mixed separately at an angular speed of (500 rad/sec) for (0.5 h); the ingot components were pressed into a cold steel mold in one direction with a different thickness of (0.2 – 0.6) cm and with a constant pressure in one direction of (600Mpa) and kept for (2 min) for each sample using a device type (HERZOG TP 20 P). [17,18].

Table 1: Samples symbol, volumetric ratio, thickness, and pressing pressure.

Code		Cu (%)	Al (%)	Ti (%)	Mo %	Zr %	P (Mpa)	T (Cm)
A	**A1**	92	5	3	-	-	600	0.2
	A2	92	5	3	-	-	600	0.3
	A3	92	5	3	-	-	600	0.4
	A4	92	5	3	-	-	600	0.5
	A5	92	5	3	-	-	600	0.6
B	**B1**	91	5	3	1	-	600	0.6
	B2	90	5	3	2	-	600	0.6
	B3	89	5	3	3	-	600	0.6
	B4	88	5	3	4	-	600	0.6
	B5	87	5	3	5	-	600	0.6
C	**C1**	91	5	3	-	1	600	0.6
	C2	90	5	3	-	2	600	0.6
	C3	89	5	3	-	3	600	0.6
	C4	88	5	3	-	4	600	0.6
	C5	87	5	3	-	5	600	0.6

2- Analysis (EDX) and microscopy (FeSEM)

Examinations (EDX) and (FeSEM) were performed for the samples, as Figures (1-6) show the results of the examination

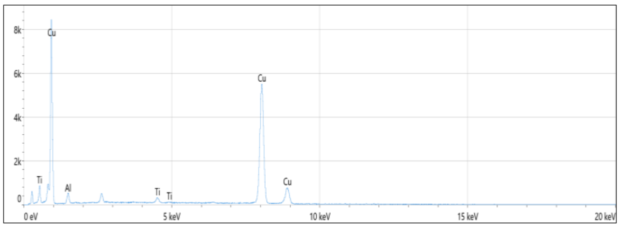

Figure1: The distribution of the elements for examination (EDX) for alloy (A5) at thickness (0.6 Cm) and compressive pressure (600Mpa).

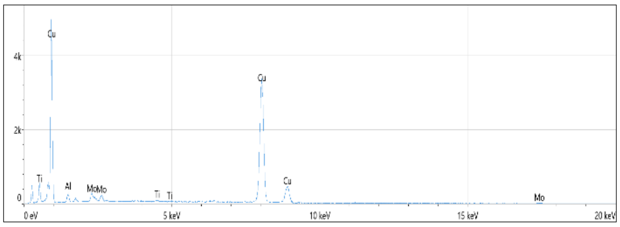

Figure 2: The distribution of the elements for examination (EDX) for alloy (B5) at thickness (0.6 Cm) and compressive pressure (600Mpa).

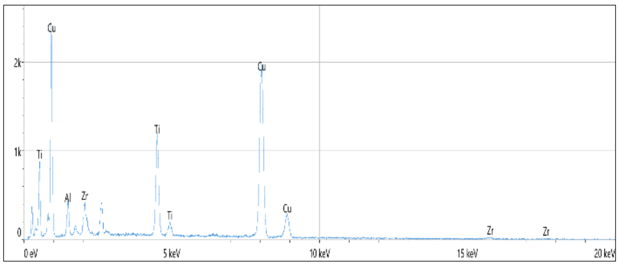

Figure 3: The distribution of the elements for examination (EDX) for alloy (C5) at thickness (0.6 Cm) and compressive pressure (600Mpa).

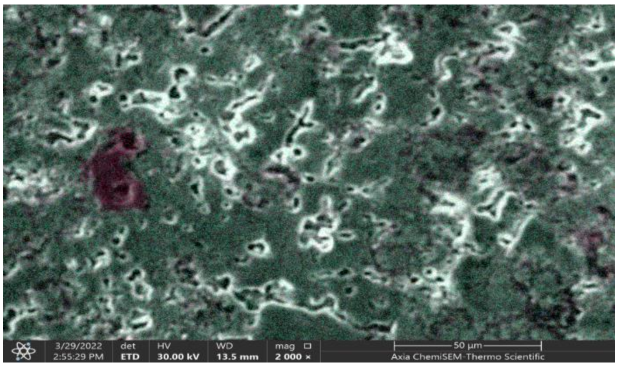

Figure 4: Scanning electron microscopy (FeSem) image of base ingot (A5) at constant pressing pressure (600Mpa).

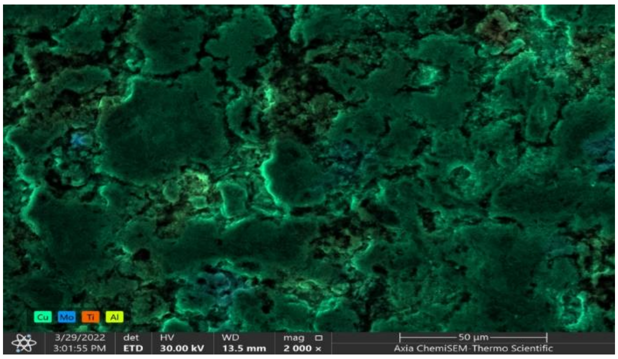

Figure 5: Scanning electron microscopy (FeSem) image of base ingot (B5) at constant pressing pressure (600Mpa).

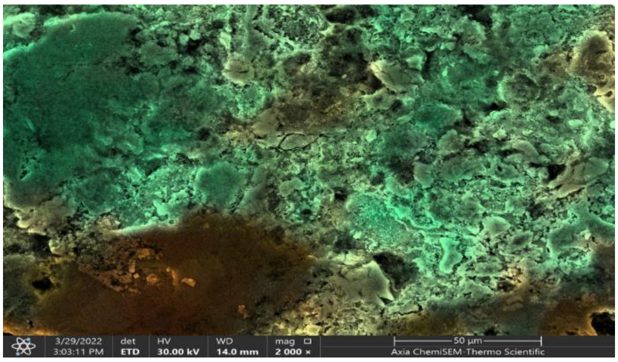

Figure 6: Scanning electron microscopy (FeSem) image of base ingot (C5) at constant pressing pressure (600Mpa).

Journal for Research in Applied Sciences and Biotechnology

www.jrasb.com

ISSN: 2583-4053

Volume-1 Issue-5 || December 2022 || PP. 188-194

https://doi.org/10.55544/jrasb.1.5.20

3- Experimental density and true porosity

Depending on the Archimedes' theory according to the international standard (ASTM B962-8), the practical density and total porosity were calculated as equations (1)(2)(3) were used to find the experimental and theoretical density and porosity of the alloys [20]:

$$\boldsymbol{E.D = \frac{Ma}{Mi-Ma}\,\rho w \,\ldots\ldots\ldots\ldots\ldots\ldots(1)}$$

$$\boldsymbol{T.D = \Sigma\,\rho i\,.Xi \,\ldots\ldots\ldots\ldots\ldots\ldots(2)}$$

$$\boldsymbol{p = \left[1 - \frac{E.D}{T.D}\right] 100\% \,\ldots\ldots\ldots\ldots(3)}$$

Since (Mα) is the weight of the sample after drying it inside the electric furnace, (Mi) is the weight of the sample. At the same time, it is suspended and immersed in distilled water, (ρw) is the density of water, (Xi) is the proportion of each element in the alloy, and (ρi) is the density of each element.

4- Hardness test

The surfaces of the samples were smoothed using graded paper of silicon carbide (800,1000,1500,2000,2500) to measure their Hardness using a Vickers hardness tester (Hv), a load of (500 gm) was applied via the stitching tool for a period of (5 sec) and the Stitching tool and measuring the diameter of the resulting effect on the surface of the sample, and the process was repeated for five times for different areas that included the surface area.

5 - X-ray diffraction (XRD)

An X-ray diffraction apparatus (SHEMADZU) XDR-6000 [9] was used.

6 - Radiation attenuation measurements

6 -1 X-rays

An X-ray device (LEYBOLD PHYWE) was used to perform attenuation measurements for the alloys under study [21].

V. RESULTS AND DISCUSSION

1- X-ray diffraction (XRD)

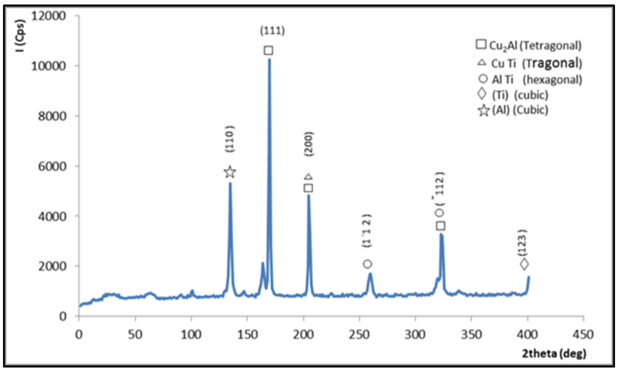

Figure 7: X-ray diffraction of (A5) alloy.

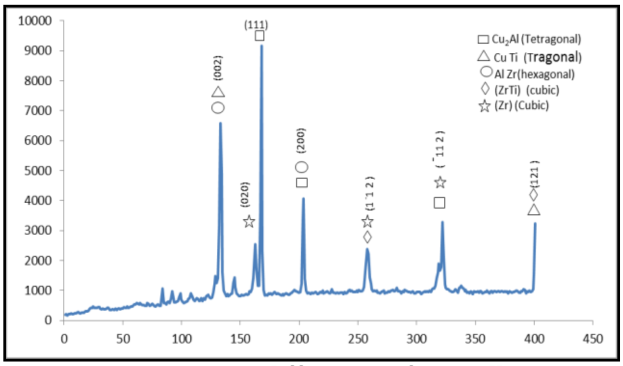

Figure 8: X-ray diffraction of (B5) alloy.

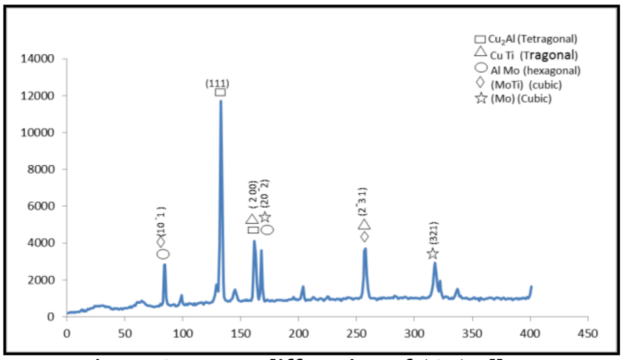

Figure 9: X-ray diffraction of (C5) alloy.

Figures (7-9) show the results of the X-ray diffraction (XRD) examination for each of the base alloys (A5) and the two alloys (B5) and (C5). The results showed the presence of elements (Cu - Al - Ti) in the base alloy and the elements (Mo, Zr) in Clear and pure for the alloys (B5, C5), as it was shown from the figures that the crystalline development of the phases and their different formations formed through data analysis had a significant impact on the results of the porosity and hardness ratios, and this is due to the addition of certain percentages of molybdenum and zirconium to the alloys.

2- Linear and mass attenuation coefficients for X-rays.

2-1 Attenuation coefficients for alloys (A1,A2,A3,A4,A5).

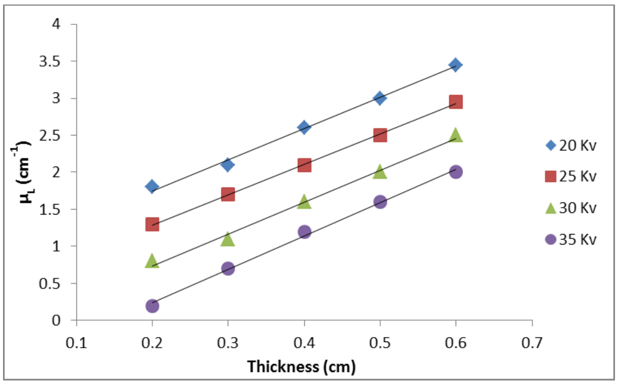

Figure 10: Relationship between linear attenuation coefficient (μL) and thickness for alloys (A1, A2, A3, A4, A5) At constant pressure (600Mpa) for a voltage range of (20,25,30,35)Kv.

ISSN: 2583-4053
Volume-1 Issue-5 || December 2022 || PP. 188-194
https://doi.org/10.55544/jrasb.1.5.20

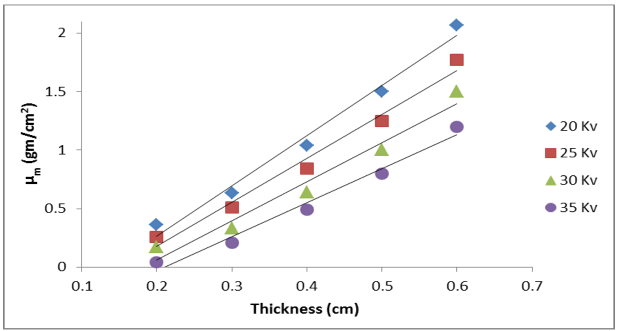

Figure 11: Relationship between mass attenuation coefficient (μm) and thickness for alloys (A1, A2, A3, A4, A5) At constant pressure (600Mpa) for a voltage range of (20,25,30,35)Kv.

Figure (10) shows that the relationship is direct between the linear attenuation coefficient and the thickness (0.2, 0.3, 0.4, 0.5, 0.6) Cm for the base alloy (Cu-Al -Ti) at a constant pressing pressure (600 Mpa) and for a range of operating voltages (20 , 35, 30, 25) Kv It was found that the best thickness of the base alloy is (0.6 cm), which represents alloy (A5), as this alloy is considered the best alloy for X-ray attenuation, and the linear attenuation coefficient increases by (47%) when comparing the results of alloy (A1). With (A5) at operating voltage (20Kv).

Figure (11) shows the direct relationship between the mass attenuation coefficient and the thickness of the base alloys (A1, A2, A3, A4, A5), as the mass attenuation coefficient increases by (61.8%) in the same comparison, and the reason for the increase in the linear and mass attenuation coefficients is due to the increase in hardness Porosity decreases, which leads to reduced distances between atoms. It was found that the relationship is inverse between the attenuation coefficients and the operating voltage, as the linear attenuation coefficient of alloy (A5) decreased by (42%) when the operating voltage was increased from (20Kv) to (35Kv).

2-2 Linear and mass attenuation coefficients (μL, μm) for alloys (B1,B2,B3,B4,B5).

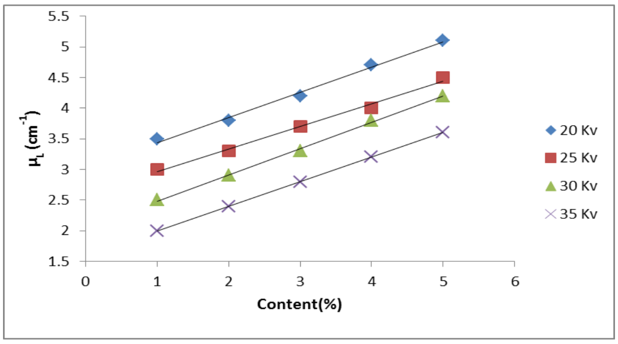

Figure 12: The relationship between the linear attenuation coefficient (μL) and the added percentages of molybdenum for alloys (B1, B2, B3, B4, B5) at a thickness of (0.6 cm) for the voltage range (20, 30, 30, 35) Kv.

Figure (12) shows the relationship between the linear attenuation coefficient and the added percentages of the molybdenum element for alloys (B1, B2, B3, B4, B5). If the relationship was found to be direct, the linear attenuation coefficient increased by (31.3%) when comparing the results of (B1) with (B5). It was found that the best addition ratio for the molybdenum element is (5%) represented by the alloy (B5), as this ratio leads to filling the voids, which leads to an increase in the practical density and the hardness ratio, In addition to a decrease in the porosity value.

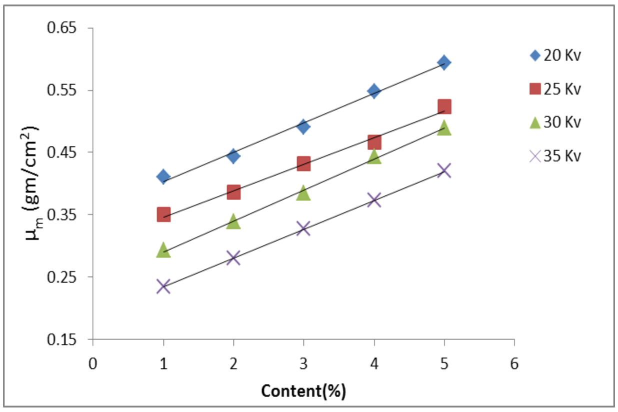

Figure 13: The relationship between the mass attenuation coefficient (μm) and the molybdenum ratios for alloys (B1, B2, B3, B4, B5) at thickness (0.6 cm) for the voltage range (20,25,30,35)Kv.

Figure (13) shows the relationship between the mass attenuation coefficient and the added percentages of the molybdenum element represented by alloys (B1, B2, B3, B4, B5), as the relationship is direct, as the mass attenuation coefficient increases by (30%) when increasing the percentages from (1 -5) %.

2-3 Linear and mass attenuation coefficients (μL, μm) for alloys (C1,C2,C3,C4,C5).

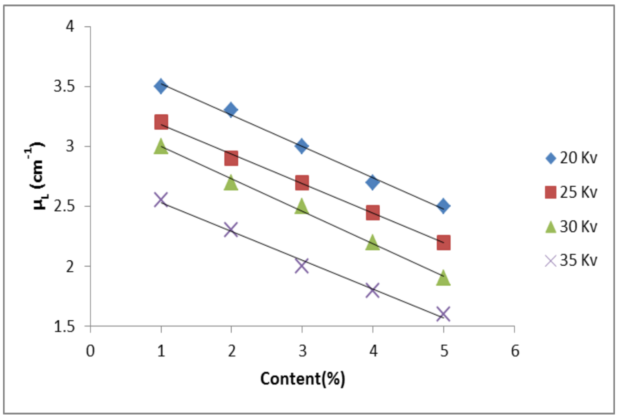

Figure 15: The relationship between the linear attenuation coefficient (μL) and the percentages of zirconium for alloys (C1, C2, C3, C4, C5) at a thickness of (0.6 cm) for a voltage range of (20,25,30,35)Kv.

ISSN: 2583-4053

Volume-1 Issue-5 || December 2022 || PP. 188-194

https://doi.org/10.55544/jrasb.1.5.20

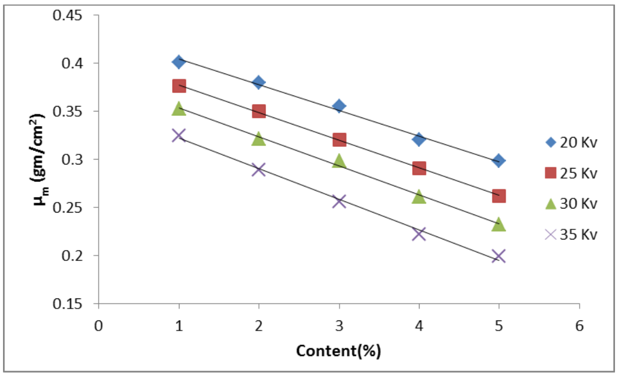

Figure 15: The relationship between the mass attenuation coefficient (µM) and the percentages of zirconium for alloys (C1, C2, C3, C4, C5) At a thickness of (0.6 cm) for a voltage range of (20,25,30,35) Kv.

Figure (14) shows the relationship between the linear attenuation coefficients and the percentages of the element zirconium represented by alloys (C1, C2, C3, C4, C5) at a constant thickness (0.6 Cm) and a constant pressing pressure (600 Mpa). Linear attenuation by (28.5%) when increasing the zirconium content of alloy (C1) to alloy (C5). Increased porosity results.

Figure (15) shows the inverse relationship between the mass attenuation coefficient and the percentages of zirconium added to the alloys (C1, C2, C3, C4, C5), as the mass attenuation coefficient decreases by (25.6%) when the zirconium content is increased from (1-5) %.

VI. CONCLUSIONS

1- The porosity decreases by (13.3%) and the hardness increases by (30%) when the thickness is increased by cm (0.2 - 0.6) for the base alloys.

2- When comparing the results of the porosity of alloys (B1) with (B5), it decreased by (33.5%), while the Hardness increased by (22.3%). When comparing the results of alloy (C1) with (C5), the porosity increased by (15%) and the Hardness decreased by (11.4%)

3- The linear and mass attenuation coefficients increase by (47%) (61.8%) when comparing the results of (A5) at a thickness of (0.6cm) with (A1) at a thickness of (0.2cm) and by (31.3%) (30%) when comparing the results. The results of (B5) alloys with (B1) are reduced when comparing the attenuation results for (C1) with (C5) alloys in the proportions (28.5%) (25.6%) at (20 Kv) voltage.

4- The attenuation coefficients decrease with the increase in the operating voltage (20-35) Kv for the X-rays, as they decreased by (29.4%) for alloy (B5) and by (36%) for alloy (C5), as when the operating voltage is increased, the intensity and intensity of the X-ray photons increases. This leads to an increase in the number of photons that penetrate the alloy.

5- The best linear and mass attenuation coefficient for (B5) alloy [Cu +5%Al +3%Ti +5%Mo] at (20Kv) with increased Hardness and decreased porosity when compared with the results of (A5) alloys (C5).

REFERENCES

[1] C.Q. Tran, C.T. Chantler, Z. Barnea, D. Paterson and D. J. Cookson, (2003) "Measurement of The X-ray Mass Attenuation Coefficient and the imaginary Part of the form Factor of Silicon Using Synchrotron Radiation" Phys. Rev. A 67 042716/1-12.

[2] D. W. Lindle, L. J. Medhurst, P. A. Heimann, M. N. Piancastelli, S. H. Liu and D.A. Shirley, (1988) "Angle-Resolved Photoemission from The Ar 2p Sub Shell" Phys. Rev. A 28 2371-4.

[3] D.C. Creagh and J.H. Hubbell, (1987) "Problems Associated with The Measurement of X-ray Attention Coefficients: I. Silicon. Report on The International Union of Crystallography X-ray Attenuation Project" ActaCrystallogr.43 102— 12.

[4] W. Dachun, D. Xunliang, W. Xinfu, Y. Hua, Z. Hongyu, S. Xinyin and Z. Guanghua, (1992) "X-ray Attenuation Coefficients and Photoelectric Cross Sections of Cu and Fe in the range 3 kev to 29 keV" Nucl. Instrum. Methods B 71 241—8.

[5] Al-Zuhairi Firas Farhan Sayed, (2001) Study of the effect of metallic paint on the resistance of Nickel alloy letter what Gester, University of Technology.

[6] G.F. Knoll " Radiation Detection and measurement " 3rd edition, (2000).

[7] Mohammed, Fareed .M, Razooqi, Raed. N, Ismael, Safana. M" The effect of Grain size for Aluminum and Some of its Alloys on coefficients of x-ray" in Australian journal of applied Science, Vol. 7, Issue 2, Page 796-803, 2012.

[8] Mohammed, Fareed .M, Razooqi, Raed. N, Yusuf, Sokayna. E" effection of oxidation of some Aluminum Alloys on coefficients of x-ray" city Science journal, Vol. 1, Issue 4, Page 33-47, 2012.

[9] Mohammed, Fareed .M, Razooqi, Raed. N, Ali, Mohsen .H" Modelling the Relation between thickness and Hardness with energy Attenuation of x-ray for pure Aluminum" in Australian journal of applied Science, Vol. 5, issue 10, Page 1268-1272, 2014.

[10] Awasarmo, Vishal V. et al. " Half and tenth value layer of some shape memory alloys the energy range 122kv to 1330kv" "International Journal of Technical, Volume 2, Issue v, page 2454-2054, 2017.

[11] Dapke Gopinath. p et al. " studies on attenuation cross section parameters of some shape memory alloys in the energy range 356kev 1330kev, indian Journal of scientific research, Volume 8, Issue 1, page 23-30, 2018.

[12] Mohammed, Fareed .M, Razooqi, Raed. N, Mohammed, Mahmmod. A" " Determination of the effect of oxidation on Attenuation coefficient of x-ray by Cu, Zn and their alloys "Tikrit journal of pure Science, 2018, Vol. 23, issue 4, Page 107-117.

ISSN: 2583-4053

Volume-1 Issue-5 || December 2022 || PP. 188-194

https://doi.org/10.55544/jrasb.1.5.20

[13] Mohammed, Fareed M., Razooqi, Raed N., Marwa, Hassan .H" studying the effect of shape memory alloys as protective shields from radiation effects in terms of attenuation coefficients of x-ray" Advances in mechanics, Vol. 9, issue 3, Page 275-290, 2021.

[14] Mohammed, Fareed .M, Razooqi, Raed .N, Mahmood, Mahmed .A" study the X-ray attenuation for a voltage range(20 – 35 kv) for copper- based smart alloys by adding silver and micro – particles " journal of pharmaceutical Negative results , Vol. 13,issue 6,Page 1-10, 2022.

[15] Satish S., Malik U.S., Raju T. N.," corrosion Behavior of Cu -Zn Ni Shape Memory Alloys" Journal of minerals and material characteristics and Engineering,1, Page 49-54, 2013.

[16] Kumar PK., Lagoudas D.C. (ed)," Introduction to shape memory Alloys Springer Science + business media LLCDol: - 10.1007 / 978-0-387-47685-8-1**,** 2008.

[17] H. Masuda, K. Higashitani, H. Yoshida, "Powder Technology Handbook " CRC Press Taylor & Francis Group, Third Edition, 2006.

[18] Razooqi, Raed Najeeb, Ahmed, saad Jeper " effect of Ag nanoparticles addition on the physical and mechanical properties of (NiTi) shape memory alloys prepared by powder metallurgy" Advances in mechanics, Volume 9, Issue 2, page 163-174, 2021.

[19] Razooqi, Raed Najeeb, salh, Ahmed Ismail " the effect of mixing time and method on some properties of (Al) alloy rein forced with carbon Nanotubes "International Journal of Mechanical Engineering, Volume 7, Issue 2, page 974-1823, 2022.

[20] H. Sh. Hammood, S. S. Irhayyiml, A. Y. Awad and H. A. Abdulhadi" Influence of Multiwall Carbon Nanotube on Mechanical and Wear Properties of Copper – Iron Composite" International journal of Automotive and Mechanical Engineering, Vol. 17, Page 7570 – 7576, 2020.

[21] A.B. Chilton, J.K. Shultis, and R.E. Faw., "Principles Radiation Shielding", Prentice - Hill, Inc ,1984.